

LA-UR- 09-03972

Approved for public release;  
distribution is unlimited.

*Title:* Understanding Aging in Pentaerythritol Tetranitrate

*Author(s):* Geoffrey W. Brown (DE-1)  
Mary M. Sandstrom (DE-1)  
Anna M. Giambra (DE-1)  
Jose G. Archuleta (DE-1)  
Deirdre C. Monroe (W-6)

*Intended for:* 28th Compatibility, Aging, and Stockpile Stewardship  
Conference. Albuquerque, NM, USA, Sept. 29 - Oct 2, 2009.



Los Alamos National Laboratory, an affirmative action/equal opportunity employer, is operated by the Los Alamos National Security, LLC for the National Nuclear Security Administration of the U.S. Department of Energy under contract DE-AC52-06NA25396. By acceptance of this article, the publisher recognizes that the U.S. Government retains a nonexclusive, royalty-free license to publish or reproduce the published form of this contribution, or to allow others to do so, for U.S. Government purposes. Los Alamos National Laboratory requests that the publisher identify this article as work performed under the auspices of the U.S. Department of Energy. Los Alamos National Laboratory strongly supports academic freedom and a researcher's right to publish; as an institution, however, the Laboratory does not endorse the viewpoint of a publication or guarantee its technical correctness.

# Understanding Aging in Pentaerythritol Tetranitrate

*Geoffrey W. Brown<sup>1</sup>, Mary M. Sandstrom<sup>1</sup>, Anna M. Giambra<sup>1</sup>, Jose G. Archuleta<sup>1</sup>, Deirdre C. Monroe<sup>2</sup>*

<sup>1</sup>High Explosive Science & Technology (DE-1), MS C920

<sup>2</sup>Detonator Technology (W-6), MS P950

Los Alamos National Laboratory, Los Alamos, NM 87545, USA

contact e-mail: geoffb@lanl.gov

## Introduction

Pentaerythritol Tetranitrate (PETN) powder is commonly used in detonators because of its sensitivity and explosive power. PETN detonation is largely determined by the average PETN particle size. This is an issue for aging and storage of weapons because PETN has a relatively high vapor pressure [1] and its average particle size changes due to thermal energy input from the environment [2]. PETN aging is a well known problem although the mechanism is not well understood. It is important to understand PETN aging so that predictive models can be constructed that will benefit stockpile surveillance and lifetime extension programs.

PETN particles are known to coarsen over time at relatively low temperatures [2]. Particle coarsening requires mass redistribution since decomposition causes powders to become finer as PETN mass is lost. Two possible mechanisms for mass redistribution are vapor phase transfer via sublimation-redeposition and solid-state mass transfer through surface diffusion.

In this work we have examined PETN powders using permeability, atomic force microscopy (AFM), and optical microscopy based particle analysis. The results of these measurements lead us to a suggested coarsening mechanism that we reproduce with rudimentary simulations. The physical mechanisms used in the simulations are then used to create an empirical model of the coarsening that may be used to make predictions of PETN aging. In the future we will be measuring the vapor pressures and other physical properties of our powders to be able to make predictions using simulations [3].

## Experimental

We characterized the particle size evolution of the PETN with a Model 95 Fisher Scientific Sub-sieve Size Analyzer (FSSA). The FSSA uses permeability of a packed powder to determine average particle diameter. In our work we convert this diameter to specific surface area [4].

AFM images of unaged PETN particles were acquired with a Veeco Instruments CP-II atomic force microscope. Images were acquired in non-contact mode with silicon cantilevers having  $\sim 10$  nm radius of curvature. During each raster scan we mapped the topography of the surface, the error signal of the scanner, and the phase difference between the cantilever's oscillation drive signal and its response. Powder samples were prepared by placing PETN onto acrylate-based double sided tape on an AFM sample disk. Excess PETN was then tapped off.

We analyzed the particle size distribution (PSD) of the starting PETN using a Malvern Pharmavision 830, which is an automated particle counting optical microscope. PETN was dispersed by mixing in heptane and samples were prepared by allowing a drop of the PETN/heptane mixture to evaporate on a glass slide. Remaining agglomerates were removed from the PSD analysis with an operator-assigned maximum single particle size. The minimum

measurable particle size using this instrument is stated to be 0.7 microns although we suspect that particles below 1 micron are not effectively counted.

For PETN aging, samples of powder were sealed in Teflon-coated aluminum containers and heated in an oven. Multiple identical cans were aged simultaneously and replicates were pulled at different times for FSSA measurement to characterize the specific surface area evolution. In this work we aged PETN at 60 C and at 70 C for ~ 600 and ~ 800 hours, respectively.

## Results and Discussion

The left panel of Figure 1 shows an AFM image of a typical particle from the PETN used in this work. The rough area around the particle is the surface of the mounting tape. The steps on the surfaces of the particles are mobile at room temperature. Steps move towards the centers of particles and can be oriented primarily along the particle length or across its width. Examination of the topographic images shows that the steps always move towards higher terraces, indicating that mass is moving from the step edges toward the particle edges. By varying the time between image acquisitions, we have verified that the step motion is not induced by the AFM tip. Step speeds at room temperature are typically ~1 nm/min.

The right panel of Figure 1 shows the specific surface area evolution of our PETN at 60 C and 70 C. Each plot symbol is the average of three replicate measurements from a single container. The behavior is typical of PETN. There is an initial rapid linear drop in specific surface area followed by a slower tail region. Analysis of the tail region shows that it follows a power law dependence on time with an exponent of 0.7. Long term power law behavior is well understood from Ostwald ripening theory [5] and represents narrowing of the PSD towards its mean.

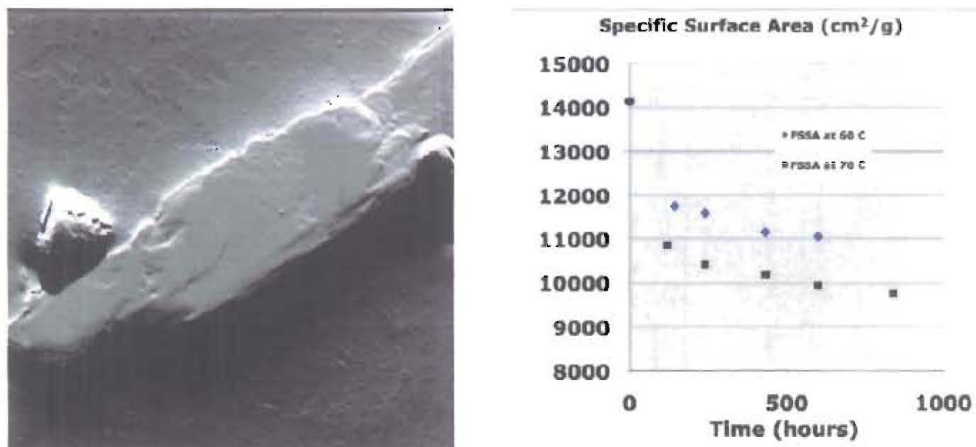


Figure 1.(left) 10  $\mu$ m AFM error signal image of large and small PETN powder particles. The rough area surrounding the particles is the mounting tape. (right) specific surface area evolution of the PETN powder used here at 60 C (blue diamonds) and 70 C (black squares).

The Pharmavision (PSD) for this PETN is shown in Figure 2. Values below 1 micron are not representative because of limitations of the optical method. We have verified this with AFM images and SEM images that show many particles in the powder with diameters below 1 micron. In addition, converting the distribution in Fig. 2 to a specific surface area yields a much lower value than the zero time value in the plot in Fig. 1.

The AFM images in figure 3 show long term particle evolution. The tape background has been digitally removed for clarity. The particle loses considerable mass over the 460 minutes that elapsed between the panels. The AFM images do not show how the mass is lost, however, we argue that it is dissolving into the mounting tape. The rate of loss is too high to be accounted for

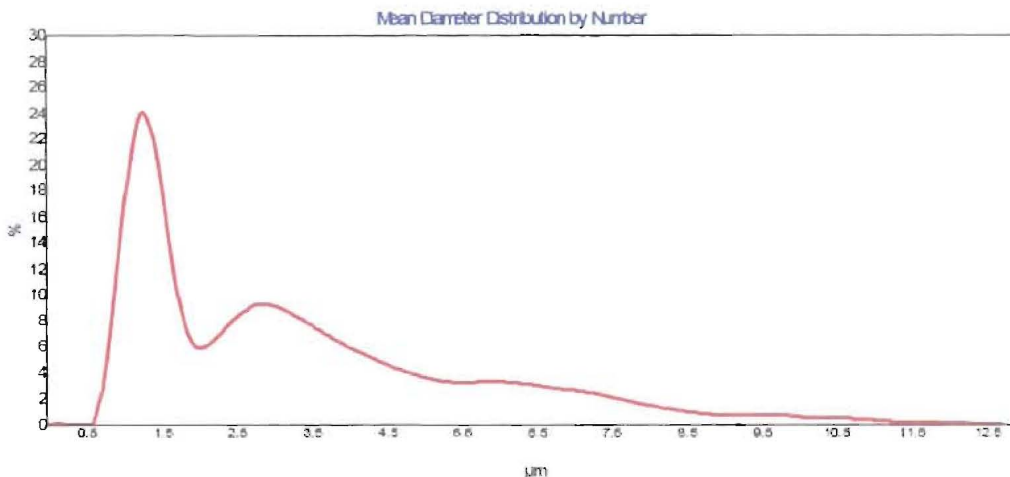


Figure 2. Particle size distribution of the PETN powder used in this study as determined by automated optical microscope inspection. Values below 1 micron are not representative due to magnification limitations.

by sublimation, which has been observed in other AFM studies [6] and can be calculated from a range of published vapor pressures [1]. In addition, it is well known that small nitrates readily dissolve into acrylate-based adhesives – this is the basis for transdermal patch delivery of certain pharmaceuticals. Our conclusion is that the mounting tape is acting as an infinite mass sink for the PETN particle. Molecules thermally detach from step edges and are removed from the particle when they reach the tape instead of redepositing on another step edge. Our mounting tape is then driving rapid mass loss at room temperature that is activated by detachment of PETN from step edges. This would not occur in a loose powder since there are no sinks. Mass will move on the surface, but will eventually either sublime or reattach to a step edge.

Redistribution of PETN must occur due to sublimation and surface mass diffusion since each is thermally activated. Sublimation can occur directly from step edges or from open terraces after detachment. Surface mass diffusion would also occur along step edges or across open terraces after detachment. We argue that our AFM images favor sublimation for mass redistribution because PETN reattachment to step edges is not observed. Steps continually move in one direction and particles continually shrink. If surface mass diffusion were to play a significant role in mass redistribution, we should see it occurring. Instead, our images indicate that PETN remains mobile until it is lost from the particle. This favors a sublimation-redeposition mechanism for coarsening.

Based on these arguments, we carried out basic simulations of sublimation-redeposition. We treated all particles as spheres and produced a starting set of particle diameters that was qualitatively similar to the PSD in Figure 3. We then added distributions of particles peaked at 0.25 and 0.5 micron diameter to bring the overall specific surface area of our model powder closer to the starting value in Figure 1. The algorithm we iterated on this PSD consisted of 1) a sublimation step to remove mass from each particle, 2) a corresponding increase in PETN background pressure, 3) a redeposition step based on kinetic theory with this background pressure as input, and 4) a subsequent decrease in the PETN background pressure. The time steps of the iteration were chosen so that the 0.25 micron particles lasted for at least  $\sim 100$  iterations at 70 C.

Loss of mass from each particle during the sublimation step is governed by a vapor pressure, or equivalently by an activation energy and attempt frequency. For a distribution with very small particles, the sublimation must take into account the Kelvin effect [7] in which the radius of curvature influences the sublimation rate. In a simple picture, a particle with a smaller diameter

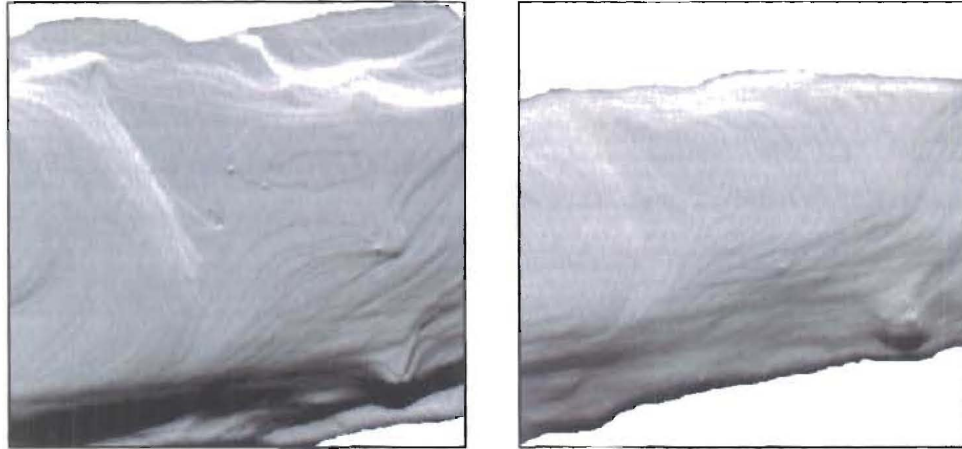


Figure 3. Left: Initial AFM phase image of a PETN powder particle. Right: AFM phase image of the same particle after 460 minutes at room temperature. The mounting tape structure has been digitally removed from these images for clarity. Image sizes are both 1.5  $\mu\text{m}$  by 1.5  $\mu\text{m}$ .

(higher curvature) has a higher step density which can lead to faster sublimation since particles at step edges are less tightly bound. The equation governing the sublimation process and mass loss per unit area in each step can then be written

$$\Delta m_- = p_\infty(T) \exp\left(\frac{C}{Tr}\right) \sqrt{\frac{M}{2\pi RT}} \Delta t \quad (1)$$

Where  $p_\infty(T)$  is the vapor pressure of very large PETN particles,  $C$  is a constant that includes the radius of curvature of the particle,  $M$  is the molecular mass, and  $R$  is the gas constant.

Redeposition from the gas phase is based on kinetic theory. Since the incident collision rate and sticking coefficient would be the same for all particle sizes, there is no dependence on particle diameter. The mass gain for each particle can be written

$$\Delta m_+ = p \sqrt{\frac{M}{2\pi RT}} \Delta t \quad (2)$$

Where  $p$  is the background PETN partial pressure.

As noted above, we do not know the vapor pressure of our powder nor do we have a quantitative measure of the PSD below 1 micron, but we can examine qualitative evolution. Iterating these equations to simulate mass loss in our model particle distribution leads the behavior shown in the left panel of Figure 4. At 60  $^\circ\text{C}$  and 70  $^\circ\text{C}$  we reproduce the initial linear region and slow tail at longer times. The slight downturn in the 70  $^\circ\text{C}$  plot is an artifact of limitations on the number of particles used in the simulation. The behavior qualitatively reproduces the observed evolution including the long term power law behavior.

Since this suggests that we understand the primary mechanism, we construct an empirical model of the coarsening from a piecewise function that includes a linear initial part (since sublimation from the smallest particles dominates at early times) and an Ostwald ripening-based power law tail. Schematically this is

$$\begin{aligned} FSSA &= At & \text{for } t < t' \\ &= Bt^D & \text{for } t > t' \end{aligned} \quad (3)$$

Where  $A$ ,  $B$ ,  $D$ , and the crossover point  $t'$  are all fit to the experimental data at 60 C and 70 C. The results are shown in the right panel of Figure 4. This will be used to determine how the coefficients change with temperature so that predictions below 60 C can be made.

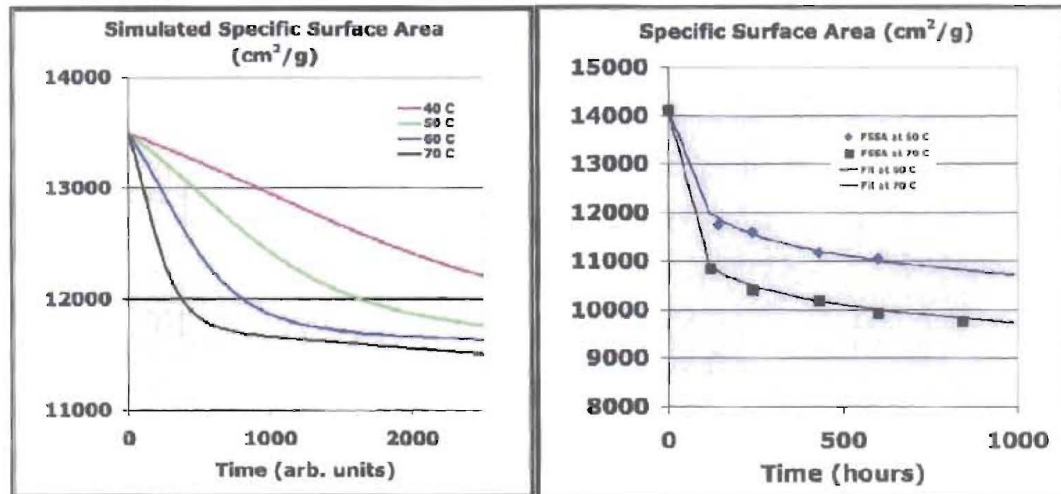


Figure 4. (left) Simulation results using the algorithm and equations listed in the text. Curves from top to bottom are for 40 C, 50 C, 60 C, and 70 C, respectively. (right) The result of fitting the data in Figure 1 with Eq. 3 at 60 C (blue diamonds) and 70 C (black squares).

### Conclusions

We have used atomic force microscopy, permeability measurements and optical microscopy to study particle coarsening in PETN powder. The results suggest that sublimation-redeposition is the mechanism of coarsening and we have qualitatively reproduced PETN specific surface area evolution with a simulation based on this mechanism. The simulation results are used to formulate an empirical model of coarsening that can be fit to the data. This empirical model can be used to predict aging at other temperatures.

### Acknowledgement.

This work was funded by Los Alamos National Laboratory's Enhanced Surveillance Campaign.

### References

- [1] G. Edwards, Trans. Faraday Soc., **1953**, *49*, 152; K.H. Lau et. al., J. Chem. Eng. Data **2004**, *49*, 544.
- [2] A. Duncan, Mason & Hanger-Silas Mason Co Report no. MHSMP-72-21, **1972**.
- [3] M.M. Sandstrom, G.W. Brown, and D.C. Monroe, This proceedings.
- [4] "Fisher Model 95 Sub-Sieve Sizer Manual", Catalog 14-311, Fisher Scientific Co., Pittsburgh, PA.
- [5] L. Shi and D.O. Northwood, Phys. Stat. Sol. (a), **1992**, *133*, K1.
- [6] R. Pitchimani, A.K. Burnham, and B.L. Weeks, J. Phys. Chem., **2007**, *111*, 9182.
- [7] S.W. Thomson, Phil. Mag., **1871**, *4*, 448.